# Effects of $CO_2$ dilution on autoignition and detonation development induced by hot spot in n-heptane/air mixtures

Peng Dai [1], Zheng Chen [2,3], Xiaohua Gan [1]
[1] Department of Mechanics and Aerospace Engineering, Southern University of Science and Technology, Shenzhen 518055, China
[2] SKLTCS, CAPT, College of Engineering, Peking University, Beijing 100871, China
[3] Beijing Innovation Center for Engineering Science and Advanced Technology, Peking University, Beijing 100871, China

## 1 Introduction

Diluted combustion is widely used in advanced internal combustion engines (ICEs) such as homogeneous charge compression ignition (HCCI) engines, low temperature combustion (LTC) engines, and engines utilizing exhaust gas recirculation (EGR) due to its advantage of reducing both NOx emission and fuel consumption [1, 2]. However, reactivity non-uniformity in these engines is inevitable and may induce localized autoignition and detonation development [3, 4]. This may lead to knock or even super-knock, especially under boosted environment. Therefore, fundamental understanding of end-gas autoignition and detonation development induced by reactivity non-uniformity under diluted condition is needed.

The pioneering work on autoignition with reactivity non-uniformity was conducted by Zel'dovich [5, 6] who proposed that different autoignition modes including detonation development may be induced by a hot spot. The theory was confirmed and extended by simulations considering simplified [7-9] or detailed chemical mechanisms [10-17]. Among them, Bradley and co-workers [10, 11] identified a detonation peninsular based on two non-dimensional parameters: the normalized temperature gradient, $\xi$, and the ratio of acoustic time to excitation time, $\varepsilon$. In our work [13, 14] detonation development regimes were identified in $\xi$-$\varepsilon$ diagram for large hydrocarbons with low-temperature chemistry. The detonation peninsular was widely used in studies related to engine knock [18-23]. For examples, Bates et al. [21] quantitatively analyzed different engine conditions corresponding to regimes from benign autoignition to super-knock; Robert et al. [23] investigated various scenarios for knock and super-knock by using LES; Recently, we have introduced a new non-dimensional parameter, $\xi_a$, to quantify regimes of different autoignition modes [15]. The new parameter $\xi_a$ is based on the transient autoignition front propagation speed and it is more suitable in describing different autoignition modes [15].

However, there are few studies on detonation development induced by reactivity gradient under diluted conditions [16, 17]. Under more diluted condition, the excitation time becomes longer and the volumetric energy density is lower. Consequently, the pressure wave and its interaction with chemical reaction both become weaker and thereby the propensity of detonation development may be reduced. Therefore, the objectives of this study are (1) to assess and interpret the effects of $CO_2$ dilution on

Correspondence to: daip@sustc.edu.cn

autoignition and detonation development induced by a hot spot in n-heptane/air mixture, and (2) to evaluate the performance of different parameters in terms of quantitatively describing autoignition modes under different conditions.

## 2 Model and specifications

The transient autoignition process initiated by a hot spot at the center of a 1-D, adiabatic, closed, spherical chamber with radius $R_w$=4 cm is investigated in this study. The hot spot with radius $r_0$ is characterized by a linear temperature distribution with negative gradient $(dT/dr)_i$. The initial temperature outside of the hot spot is $T_{i,0}$=1000 K and the initial n-heptane/air/$CO_2$ mixture composition in the chamber is stoichiometric with specified $CO_2$ dilution ratio, $c_{CO2}$. The mixture is initially static (i.e., $u$=0 m/s) at $P_0$=40 atm.

The 1-D autoignition process is simulated using the in-house code A-SURF [24, 25] which uses a multi-level, dynamically adaptive mesh refinement algorithm to maintain adequate numerical resolution of the reaction zone, pressure wave, shock wave, and detonation wave. The skeletal mechanism for n-heptane oxidation [26] is used in simulation. It has been demonstrated to be able to accurately predict ignition and flame propagation in n-heptane/air mixture at a broad range of temperature, pressure and equivalence ratio [26].

## 3 Results and Discussion

0-D homogeneous ignition of n-heptane/air/$CO_2$ mixture at constant volume is first investigated. Figure 1 shows the influence of $CO_2$ dilution on the ignition delay time and excitation time, which are defined as the time for maximum heat release rate and the time interval between 5% and maximum heat release rate, respectively. It is seen that both $\tau$ and $\tau_e$ increase with increasing $c_{CO2}$, while the latter is much more sensitive to $c_{CO2}$. This indicates that the major ignition heat releasing process can be significantly mitigated under more diluted condition.

For the hot spot, there is a critical temperature gradient at which the theoretical autoignition front propagation speed, $u_a$, is equal to the sound speed, $a$, which is defined as [6, 11]:

$$\left(dT/dr\right)_c = \left(a\left(d\tau/dT_0\right)\right)^{-1} \tag{1}$$

The critical temperature gradient is also plotted in Fig. 1 which indicates that the autoignition mode may change when the mixture becomes more diluted.

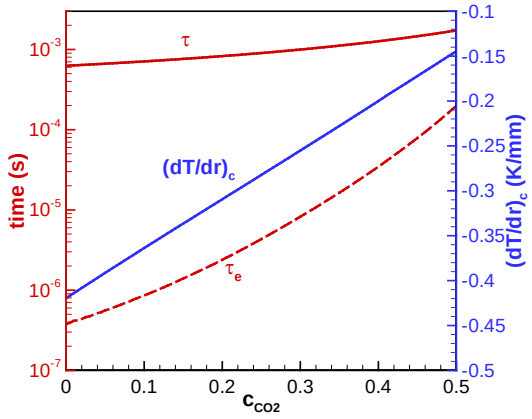


Fig. 1 Change of 0-D ignition delay time, excitation time and critical temperature gradient with $CO_2$ molar fraction in stoichiometric n-heptane/air mixture at $T_0$=1000 K and $P_0$=40 atm.

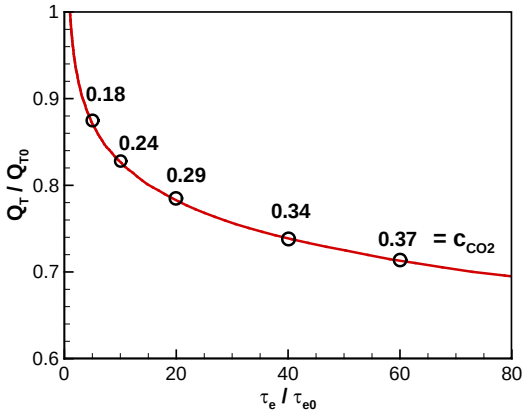


Fig. 2 Change of total heat release during 0-D ignition with the corresponding excitation time, which are respectively normalized by the values of undiluted mixture (i.e., $Q_{T0}$ and $\tau_{e0}$ at $c_{CO2}$=0).

In addtion, Fig. 2 shows that with the increase of $CO_2$ dilution, the excitation time becomes longer and the volumetric energy density is lower. Consequently, it is expected that the pressure wave and its interaction with chemical reaction both become weaker and thereby the propensity of detonation development becomes lower.

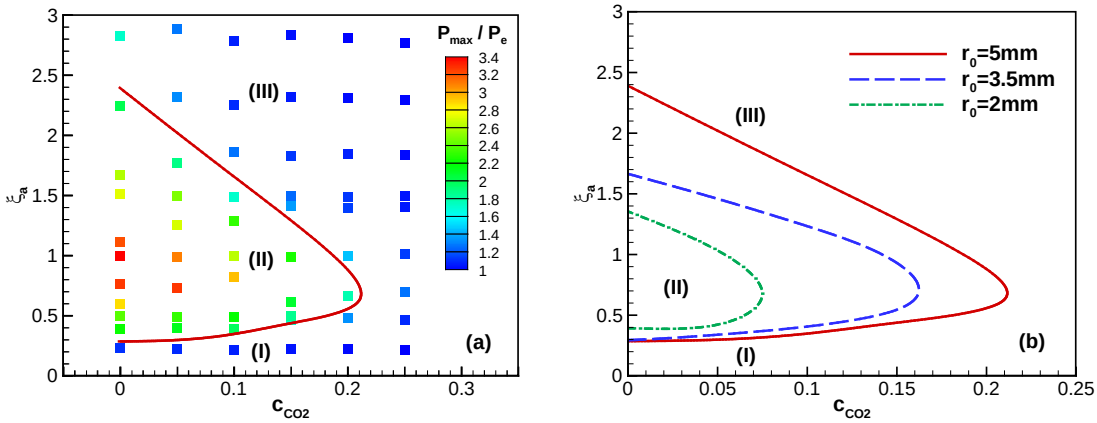


Fig. 3 Regimes of autoignition modes induced by a hot spot of (a) $r_0$= 5 mm and (b) different radii in stoichiometric n-heptane/air with different amounts of $CO_2$ dilution. The three autoignition modes are (I) supersonic reaction front propagation, (II) detonation development, and (III) subsonic reaction front propagation, respectively. The maximum pressure, $P_{max}$, in sub-figure (a) is normalized by the equilibrium value of 0-D constant-volume ignition, $P_e$.

The 1-D autoignition front propagation process induced by a hot spot is simulated at different $CO_2$ dilution ratios. It is noted that the theoretical autoignition front propagation speed, $u_a=a/\xi$, which is calculated based on the initial temperature gradient [11], usually differs from the actual transient autoignition front propagation speed, denoted as $S$, due to the impact of thermal/mass diffusion transport around the hot spot during induction period. Therefore, in Ref. [15] we introduced another non-dimensional parameter, $\xi_a$, based on the actual autoignition front propagation speed:

$$\xi_a = a_{r_0/2} \big/ S_{AVG} \tag{2}$$

where $a_{r0/2}$ and $S_{AVG}$ are respectively the sound speed at $r=r_0/2$ and the average speed of autoignition front propagating within the hot spot (i.e., $0 \le r \le r_0$) calculated from 1-D simulation. It was demonstrated that $\xi_a$ increases monotonously with $\xi$ and that the detonation development regime can be better quantified in the $\xi_a$-$\varepsilon$ diagram than in the $\xi$-$\varepsilon$ diagram since $\xi_a$ can better evaluate the interaction between the actual propagating autoignition front and pressure wave [15].

Figure 3(a) summarizes the autoignition modes for $r_0$=5 mm in $\xi_a$-$c_{CO2}$ diagram. The maximum pressure, $P_{max}$, normalized by its equilibrium value for 0-D constant-volume ignition, $P_e$, is shown for each case. With the increase of $\xi_a$, three autoignition modes can be sequentially identified, which are similar to those observed in our previous studies [14, 15], namely: (I) supersonic reaction front propagation, (II) detonation development, and (III) subsonic reaction front propagation. It is seen in Fig. 3(a) that the detonation development occurs within a reversed C-shaped regime in the $\xi_a$-$c_{CO2}$ diagram. This indicates that detonation development becomes more difficult at higher $CO_2$ dilution. For $c_{CO2} \ge 0.2$, the hot spot cannot induce detonation development. Therefore, detonation development and super-knock may be prevented when high EGR is used. Figure 3(b) shows the results for different hot spot sizes of $r_0$=2, 3.5 and 5 mm. It is observed that the detonation development regime is narrower for smaller hot spot size, implying that it is more difficult to achieve detonation development for a smaller hot spot. This is mainly

because the total chemical energy deposited into the developing pressure wave within the hot spot is reduced as $r_0$ decreases [11, 13].

By examining typical autoignition cases with different $c_{CO2}$ and $r_0$, it is found that the excitation time and hot spot size play dominating roles in the chemical-acoustic interaction process during autoignition at given value of $\xi_a$. The effects of hot spot size are also clearly demonstrated in Fig. 3. By introducing the paramter $\varepsilon$ which is defined as the ratio between the acoustic time, $r_0/a$, and excitation time, $\tau_e$ (i.e. $\varepsilon=r_0/(a\tau_e)$) [11], the results in Fig. 3(b) are plotted in the $\xi_a$-$\varepsilon$ diagram as shown in Fig. 4. It is seen that the detonation limits represented by the C-shaped curves are almost unaffected by $r_0$. This indicates that $\varepsilon$ can well quantify different autoignition modes by comprehensively assessing the impact of chemical energy deposition into developing pressure wave within the hot spot.

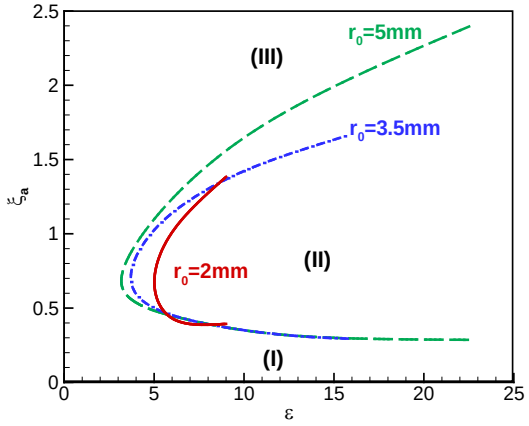


Fig. 4 Regimes of autoignition modes induced by a hot spot with different radii in $CO_2$ diluted n-heptane/air mixtures.

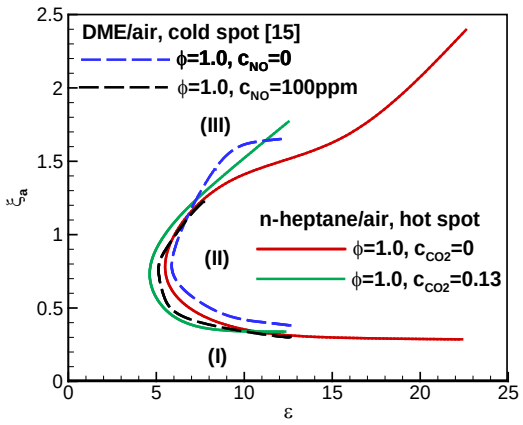


Fig. 5 Regimes of autoignition modes induced by a hot spot in n-heptane/air/$CO_2$ mixtures at $T_{i,0}$=1000 K and $P_0$=40 atm and by a cold spot in DME/air/NO mixtures at $T_{i,0}$=975 K and $P_0$=40 atm [15].

The above-mentioned detonation limits are obtained by changing the $CO_2$ concentration at a specified hot spot size. Detonation limits in terms of varying hot spot size (i.e. $r_0$=1~8 mm) at specified mixture compositions are also identified, and the results are plotted in Fig. 5. The undiluted ($c_{CO2}$=0) and diluted ($c_{CO2}$=0.13) mixture are considered. Moreover, limits of detonation development regime induced by cold spot in dimethyl ether (DME)/air mixture with NO addition from Ref. [15] are also plotted together for comparison. It is seen that the detonation limits for different mixture compositions and initial conditions quantitatively agree with one another in the $\xi_a$-$\varepsilon$ diagram while there are obvious discrepancies among those in $\xi$-$\varepsilon$ diagram (not shown here due to space limit). Therefore, parameter $\xi_a$ is better than $\xi$ in terms of quantitatively describing detonation development regime. Furthermore, Fig. 5 shows that the low-temperature chemistry (i.e. in cases with cold spot for DME/air) has negligible effect on the detonation development regime in $\xi_a$-$\varepsilon$ diagram. This is mainly due to the fact that the reaction front propagation is driven by the main portion of heat release at high temperatures and that low-temperature chemistry only has secondary influence on the chemical-acoustic interaction. The detonation development regimes for n-heptane/air/$CO_2$ mixtures shown in Fig. 5 are also compared with those in Fig. 4, and quantitative agreement is achieved among those detonation limts under different conditions. This indicates that the main physical-chemical factors affecting autoignition process can be adequately represented by the two parameters, $\xi_a$ and $\varepsilon$.

## 4 Conclusions

The effects of $CO_2$ dilution on autoignition modes induced by a hot spot in n-heptane/air mixture is numerically investigated considering detailed chemistry. It is found that the increase of $CO_2$ dilution can greatly increase the excitation time and reduce volumetric energy density. Therefore, the propensity of detonation development becomes lower since the pressure wave and its interaction with chemical reaction both become weaker under more diluted condition. The $\xi_a$-$c_{CO2}$ and $\xi_a$-$\varepsilon$ diagrams are introduced to quantitatively describe different autoignition modes including detonation development. The corresponding detonation limits are observed to quantitatively agree with one another under various conditions in $\xi_a$-$\varepsilon$ diagram, indicating that the main physical-chemical factors affecting autoignition process can be adequately represented by $\xi_a$ and $\varepsilon$.

## Acknowledgements

This work is supported by National Natural Science Foundation of China (Nos. 51606091 and 91741126).

## References

[1] Putrasari Y, Jamsran N, Lim O. (2017). An investigation on the DME HCCI autoignition under EGR and boosted operation. Fuel 200: 447-457.
[2] Cung K, Moiz AA, Zhu XC, Lee SY. (2017). Ignition and formaldehyde formation in dimethyl ether (DME) reacting spray under various EGR levels. Proc. Combust. Inst. 36: 3605-3612.
[3] Nygren J, Hult J, Richter M, Alden M, Christensen M, Hultqvist A, Johansson B. (2002). Three-dimensional laser induced fluorescence of fuel distributions in an HCCI engine. Proc. Combust. Inst. 29: 679-685.
[4] Wang Z, Qi Y, He X, Wang J, Shuai S, Law CK. (2015). Analysis of pre-ignition to super-knock: hotspot-induced deflagration to detonation. Fuel 144: 222-227.
[5] Zeldovich YB, Librovich VB, Makhviladze GM, Sivashinsky GI. (1970). On the development of detonation in non-uniformly preheated gas. Acta Astronaut 15: 313-321.
[6] Zeldovich YB. (1980). Regime Classification of an Exothermic Reaction with Nonuniform Initial Conditions. Combust. Flame 39: 211-214.
[7] Sharpe GJ, Short M. (2003). Detonation ignition from a temperature gradient for a two-step chain-branching kinetics model. J. Fluid Mech. 476: 267-292.
[8] Kurtz MD, Regele JD. (2014). Acoustic timescale characterisation of a one-dimensional model hot spot. Combust. Theory Model. 18: 532-551.
[9] Misdariis A, Vermorel O, Poinsot T. (2015). A methodology based on reduced schemes to compute autoignition and propagation in internal combustion engines. Proc. Combust. Inst. 35: 3001-3008.
[10] Bradley D, Morley C, Gu XJ, Emerson DR. (2002). Amplified pressure waves during autoignition: relevance to CAI engines. SAE Technical Paper, 2002-01-2868.
[11] Gu XJ, Emerson DR, Bradley D. (2003). Modes of reaction front propagation from hot spots. Combust. Flame 133: 63-74.
[12] Liberman MA, Kiverin AD, Ivanov MF. (2011). On detonation initiation by a temperature gradient for a detailed chemical reaction models. Phys. Lett. A 375: 1803-1808.
[13] Dai P, Chen Z, Chen SY, Ju YG. (2015). Numerical experiments on reaction front propagation in n-heptane/air mixture with temperature gradient. Proc. Combust. Inst. 35: 3045-3052.

[14] Dai P, Qi CK, Chen Z. (2017). Effects of initial temperature on autoignition and detonation development in dimethyl ether/air mixtures with temperature gradient. Proc. Combust. Inst. 36: 3643-3650.
[15] Dai P, Chen Z. (2019). Effects of NOx addition on autoignition and detonation development in DME/air under engine-relevant conditions. Proc. Combust. Inst. 37: 4813-4820.
[16] Guerouani A, Robert A, Zaccardi J-M. (2018). Detonation Peninsula for TRF-Air Mixtures: Assessment for the Analysis of Auto-Ignition Events in Spark-Ignition Engines. SAE Technical Paper, 2018-01-1721, doi:10.4271/2018-01-1721.
[17] Zander L, Tornow G, Klein R, Djordjevic N, Influence of autoignition delay time characteristics of different fuels on pressure, Active Flow and Combustion Control 2018, Springer, Cham, 2019, 151-166.
[18] Bradley D, Kalghatgi GT. (2009). Influence of autoignition delay time characteristics of different fuels on pressure waves and knock in reciprocating engines. Combust. Flame 156: 2307-2318.
[19] Kalghatgi GT, Bradley D. (2012). Pre-ignition and 'super-knock' in turbo-charged spark-ignition engines. Int. J. Engine Res. 13: 399-414.
[20] Rudloff J, Zaccardi JM, Richard S, Anderlohr JM. (2013). Analysis of pre-ignition in highly charged SI engines: Emphasis on the auto-ignition mode. Proc. Combust. Inst. 34: 2959-2967.
[21] Bates L, Bradley D, Paczko G, Peters N. (2016). Engine hot spots: Modes of auto-ignition and reaction propagation. Combust. Flame 166: 80-85.
[22] Pan JY, Shu GQ, Wei HQ. (2014). Interaction of Flame Propagation and Pressure Waves during Knocking Combustion in Spark-Ignition Engines. Combust. Sci. Technol. 186: 192-209.
[23] Robert A, Richard S, Colin O, Poinsot T. (2015). LES study of deflagration to detonation mechanisms in a downsized spark ignition engine. Combust. Flame 162: 2788-2807.
[24] Chen Z, Burke MP, Ju YG. (2009). Effects of Lewis number and ignition energy on the determination of laminar flame speed using propagating spherical flames. Proc. Combust. Inst. 32: 1253-1260.
[25] Chen Z. (2010). Effects of radiation and compression on propagating spherical flames of methane/air mixtures near the lean flammability limit. Combust. Flame 157: 2267-2276.
[26] Liu SL, Hewson JC, Chen JH, Pitsch H. (2004). Effects of strain rate on high-pressure nonpremixed n-heptane autoignition in counterflow. Combust. Flame 137: 320-339.